require further exploration to determine their roles in, and possible effects on, the evolution of Cretaceous terrestrial ecosystems. □

Methods

Taxon sampling and DNA sequencing

We assembled two independent data sets (ferns and angiosperms) and used the lycophyte *Huperzia* as the outgroup (not shown in Fig. 1) for both. For ferns, we sampled the chloroplast *rbcL* and *rps4* genes for 45 taxa: 41 leptosporangiate ferns from all major lineages (focusing within the polypods), one horsetail, two seed plants, and the outgroup. For angiosperms, we sampled the chloroplast *rbcL*, *atpB* and nuclear small-subunit ribosomal DNA genes for 95 taxa (mostly a subset from data set in ref. 14): 84 angiosperms, eight gymnosperms, one leptosporangiate fern, one horsetail, and the outgroup. Most DNA sequence data were already available in GenBank; 19 new fern sequences were generated as part of this study following the DNA extraction, amplification and sequencing protocols in ref. 18, and are deposited in GenBank. For fern voucher information and GenBank accession numbers see Supplementary Information.

Phylogenetic analyses

Phylogenetic analyses using a bayesian approach were conducted separately for ferns and angiosperms with MrBayes version 3.0b4 (ref. 29). Each gene in each data set was assigned its own model of evolution (GTR + I + Γ for each gene, determined using a hierarchical likelihood ratio test approach) and analyses were conducted using four chains, run for a total of 10,000,000 generations, with trees sampled from the cold chain every 1,000 generations. The resulting 10,000 trees were plotted against their likelihoods to determine the point where the likelihoods converged on a maximum value, and all 500 trees (500,000 generations) before this convergence were discarded as the 'burn-in' phase. For each data set (ferns and angiosperms), we computed a majority-rule consensus of the remaining 9,500 trees. We used this phylogenetic hypothesis (with average branch lengths), as well as 1,000 trees randomly sampled from among the 9,500 trees, in the subsequent analyses.

Divergence time estimates

Divergence time estimates were obtained through penalized likelihood analyses (truncated Newton algorithm) of the fern and angiosperm consensus phylogenies in r8s version 1.60 (ref. 30). For each data set, fossil age constraints were applied as indicated in Table 1 (for details see Supplementary Information) and the appropriate smoothing value was determined using cross-validation. For angiosperms, fossil age constraints[22] (Table 1) were applied in two ways, differing only in the application of the fossil age of the angiosperm crown group (node b10 in Fig. 1b). The first approach was strict (age fixed at 132 Myr; ref. 22) and the second relaxed (minimum age constraint of 132 Myr applied). To evaluate the effects of phylogenetic uncertainty[21] due to both topological and branch-length estimation error, divergence times were also estimated using penalized likelihood for each of the 1,000 randomly sampled bayesian trees for each data set. Fossil age constraints were applied as described above and individual smoothing values were determined for each tree using cross-validation. The molecular age estimates for each well-supported node (posterior probability ≥0.95; therefore, 950–1,000 estimates for each node, depending on support) were averaged and the standard deviation calculated.

Lineages-through-time plots

The chronograms resulting from the penalized likelihood analyses of the consensus phylogenies were used to calculate proportional lineages-through-time plots for polypods and angiosperms. Numbers of lineages were tallied at sequential time points (10 Myr intervals) and are presented as proportions (%) of the number of polypod or angiosperm terminals.

Received 5 November 2003; accepted 22 January 2004; doi:10.1038/nature02361.

1. Crane, P. R. in *The Origin of Angiosperms and Their Biological Consequences* (eds Friis, E. M., Chaloner, W. G. & Crane, P. R.) 107–144 (Cambridge Univ. Press, Cambridge, 1987).
2. Lidgard, S. & Crane, P. R. Angiosperm diversification and Cretaceous floristic trends: A comparison of palynofloras and leaf macrofloras. *Paleobiology* **16,** 77–93 (1990).
3. Crane, P. R., Friis, E. M. & Pedersen, K. R. The origin and early diversification of angiosperms. *Nature* **374,** 27–33 (1995).
4. Lupia, R., Lidgard, S. & Crane, P. R. Comparing palynological abundance and diversity: Implications for biotic replacement during the Cretaceous angiosperm radiation. *Paleobiology* **25,** 305–340 (1999).
5. Nagalingum, N. S., Drinnan, A. N., Lupia, R. & McLoughlin, S. Fern spore diversity and abundance in Australia during the Cretaceous. *Rev. Palaeobot. Palynol.* **119,** 69–92 (2002).
6. Niklas, K. J., Tiffney, B. H. & Knoll, A. H. Patterns in vascular land plant diversification. *Nature* **303,** 614–616 (1983).
7. Smith, A. R. Comparison of fern and flowering plant distributions with some evolutionary interpretations for ferns. *Biotropica* **4,** 4–9 (1972).
8. Lovis, J. D. Evolutionary patterns and processes in ferns. *Adv. Bot. Res.* **4,** 229–415 (1977).
9. Rothwell, G. W. in *Pteridology in Perspective* (eds Camus, J. M., Gibby, M. & Johns, R. J.) 395–404 (Royal Botanic Gardens, Kew, 1996).
10. Collinson, M. E. in *Pteridology in Perspective* (eds Camus, J. M., Gibby, M. & Johns, R. J.) 349–394 (Royal Botanic Gardens, Kew, 1996).
11. Schneider, H. & Kenrick, P. An Early Cretaceous root-climbing epiphyte (Lindsaeaceae) and its significance for calibrating the diversification of polypodiaceous ferns. *Rev. Palaeobot. Palynol.* **115,** 33–41 (2001).
12. Dilcher, D. L. Paleobotany: Some aspects of non-flowering and flowering plant evolution. *Taxon* **50,** 697–711 (2001).
13. Friis, E. M., Pederson, K. R. & Crane, P. R. Fossil evidence of water lilies (Nymphaeales) in the Early Cretaceous. *Nature* **410,** 357–360 (2001).
14. Soltis, D. E. *et al.* Angiosperm phylogeny inferred from 18S rDNA, *rbcL*, and *atpB* sequences. *J. Linn. Soc. Bot.* **133,** 381–461 (2000).
15. Soltis, P. S., Soltis, D. E. & Chase, M. W. Angiosperm phylogeny inferred from multiple genes as a tool for comparative biology. *Nature* **402,** 402–404 (1999).
16. Qiu, Y.-L. *et al.* The earliest angiosperms: Evidence from mitochondrial, plastid and nuclear genomes. *Nature* **402,** 404–407 (1999).
17. Skog, J. E. Biogeography of Mesozoic leptosporangiate ferns related to extant ferns. *Brittonia* **53,** 236–269 (2001).
18. Pryer, K. M. *et al.* Horsetails and ferns are a monophyletic group and the closest living relatives to seed plants. *Nature* **409,** 618–622 (2001).
19. Deng, S. Ecology of the Early Cretaceous ferns of Northeast China. *Rev. Palaeobot. Palynol.* **119,** 93–112 (2002).
20. Sanderson, M. J. Estimating absolute rates of molecular evolution and divergence times: A penalized likelihood approach. *Mol. Biol. Evol.* **19,** 101–109 (2002).
21. Pagel, M. & Lutzoni, F. in *Biological Evolution and Statistical Physics* (eds Lässig, M. & Valleriani, A.) 148–161 (Springer, Berlin, 2002).
22. Magallón, S. & Sanderson, M. J. Absolute diversification rates in angiosperm clades. *Evolution* **55,** 1762–1780 (2001).
23. Wikström, N., Savolainen, V. & Chase, M. W. Evolution of the angiosperms: Calibrating the family tree. *Proc. R. Soc. Lond. B* **268,** 2211–2220 (2001).
24. Benton, M. J. & Ayala, F. J. Dating the Tree of Life. *Science* **300,** 1698–1700 (2003).
25. Soltis, P. S., Soltis, D. E., Savolainen, V., Crane, P. R. & Barraclough, T. G. Rate heterogeneity among lineages of tracheophytes: Integration of molecular and fossil data and evidence for molecular living fossils. *Proc. Natl Acad. Sci. USA* **99,** 4430–4435 (2002).
26. Wikström, N. & Kenrick, P. Evolution of Lycopodiaceae (Lycopsida): Estimating divergence times from *rbcL* gene sequences by use of nonparametric rate smoothing. *Mol. Phylogenet. Evol.* **19,** 177–186 (2001).
27. Kawai, H. *et al.* Responses of ferns to red light are mediated by an unconventional photoreceptor. *Nature* **421,** 287–290 (2003).
28. Smith, H. Phytochromes and light signal perception by plants—an emerging synthesis. *Nature* **407,** 585–591 (2000).
29. Huelsenbeck, J. P. & Ronquist, F. MRBAYES: Bayesian inference of phylogenetic trees. *Bioinformatics* **17,** 754–755 (2001).
30. Sanderson, M. J. r8s: Inferring absolute rates of molecular evolution and divergence times in the absence of a molecular clock. *Bioinformatics* **19,** 301–302 (2003).

Supplementary Information accompanies the paper on **www.nature.com/nature**.

Acknowledgements We thank the Duke Biology systematics discussion group, especially P. Manos, for suggestions; F. Lutzoni, N. Nagalingum and A. R. Smith for comments on the manuscript; and M. Skakuj for the thumbnail sketches included in Fig. 1. This work was supported in part by grants from the National Science Foundation to H.S., K.M.P., R.C. and R.L.; by the Deep Time Research Coordination Network (NSF); and by the A.W. Mellon Foundation Fund to Duke University for Plant Systematics.

Competing interests statement The authors declare that they have no competing financial interests.

Correspondence and requests for materials should be addressed to K.M.P. (pryer@duke.edu). Nucleotide sequences newly determined here have been deposited in GenBank under the accession numbers AY459153–AY459171.

Adaptation to natural facial categories

Michael A. Webster, Daniel Kaping, Yoko Mizokami & Paul Duhamel

Department of Psychology, University of Nevada, Reno, Nevada 89557, USA

Face perception is fundamentally important for judging the characteristics of individuals, such as identification of their gender, age, ethnicity or expression. We asked how the perception of these characteristics is influenced by the set of faces that observers are exposed to. Previous studies have shown that the appearance of a face can be biased strongly after viewing an altered image of the face, and have suggested that these after-effects reflect response changes in the neural mechanisms underlying object or face perception[1–5]. Here we show that these adaptation effects are pronounced for natural variations in faces and for natural categorical judgements about faces. This

suggests that adaptation may routinely influence face perception in normal viewing, and could have an important role in calibrating properties of face perception according to the subset of faces populating an individual's environment.

Physical differences among faces are small compared with the range of variation in many classes of non-face objects, yet observers are highly sensitive to the subtle stimulus differences distinguishing faces. A special capacity for face perception might reflect specialized neural subsystems[6–8] and expertise developed through extensive experience with faces[9,10]. Adaptation to faces transfers across differences in the size[2,3], retinal position[2] and orientation[4,5] of face images, and thus may alter sensitivity directly at these specialized levels. In this study we do not address the site of the sensitivity change, but focus on whether these changes can arise in natural viewing. Even if the after-effects of adaptation reflect more peripheral and general stages of the visual system, the adaptation could be involved centrally in shaping the properties and dynamics of face perception, if the variations among actual faces are large enough to induce different states of adaptation. To test this, we examined adaptation to actual images of faces, and how this affected the types of judgements that observers normally make when viewing faces. These judgements typically involve classifying a face image according to a specific trait or individual identity, and may involve categorical perception (perceiving the stimulus continuum in terms of relatively discrete categories) for such characteristics[11–13]. Our measurements do not test for categorical perception of faces, but instead test whether the stimulus boundaries that observers choose for different face categories can be shifted by prior adaptation.

Stimuli were formed by morphing between pairs of face images to produce a finely graded series of images spanning the two original faces. The face pairs differed in gender, ethnicity (Japanese or Caucasian) or expression (Fig. 1). Observers made forced-choice responses to categorize images along the continuum (for example, responding as to whether a face from a gender morph appeared 'female' or 'male'). These responses were used to estimate the category boundary at which either response was equally likely. We then asked how these boundaries shifted after observers viewed either of the original face images defining the categories.

The boundary for gender represents an androgynous image intermediate to the female and male exemplars, and could be set consistently by observers (relative to the magnitude of the shifts induced by adaptation). However, after adapting to a male face, the previously ambiguous image appeared distinctly female, and thus the image that now appeared neutral was shifted towards the male image (Fig. 2a). Conversely, adaptation to the female face induced the opposite changes. Differences in the gender boundaries after adaptation were assessed for each individual subject with a two-way analysis of variance (adapted face (male versus female) by test morph (three face pairs)). For all five observers, the mean settings differed significantly for male or female adaptation ($F_{1,18} \geq 23.36$, $P < 0.001$), but did not differ for the specific face pair tested ($F_{2,18} \leq 1.84$, not significant (NS)) and did not show a significant interaction between adapting condition and face pair ($F_{2,18} \leq 1.08$, NS). We found similar after-effects for each of the other face categories we examined. For example, adaptation to a Japanese or Caucasian face again significantly biased the perceived neutral image in the sequence between them ($F_{1,18} \geq 56.1$, $P < 0.001$) (Fig. 2c). These biases were large perceptually (Fig. 3), and are consistent with a shift in the perceived neutral point towards the adapting image, because the adapting face itself appears more neutral. That is, the adaptation may re-centre the 'face space' relative to the adapting facial configuration.

Could observers adapt to the stimulus differences defining traits like gender in the male and female face pairs or only to the differences defining individual identity? To assess this we adapted subjects to a collection of ten male or ten female faces, each displayed as a random sequence of faces changing every 250 ms during the adaptation intervals. We then measured the gender boundary along male–female image arrays for face images that were not part of the adapting set (Fig. 2b). Once again the category boundaries were significantly biased by adaptation ($F_{1,18} \geq 8.55$; $P < 0.01$). This suggests that the set of faces shared common characteristics plausibly related to their common gender, and that these induced adaptation to the attribute of gender, which transferred to the perception of new individuals. Similarly, adaptation to distortions that alter the rated attractiveness of one set of faces influences the perceived attractiveness of a different set of faces[4].

Judgements of ethnicity and gender reflect distinctions between individuals. We also examined whether adaptation influenced how variations within a single face are categorized, by measuring the perceived expression of a face. Facial expressions involve an innate and universal pattern of behaviour, and are perceived in terms of a small number of relatively discrete categories (for example, angry, happy or surprised)[14]. We morphed between different pairs of expressions in a single face[15], and then determined the stimulus boundary between these pairs before or after adapting to the original expression. The after-effects of adaptation were consistent with those we found for gender and ethnicity (Fig. 2d). For example, in a happy–angry morph, previous adaptation to the angry or happy face induced clear differences in the expression boundary ($F_{1,6} \geq 9.71$, $P < 0.05$). Similar shifts in the neutral point after adaptation occurred in morphs between disgust–surprise ($F_{1,6} \geq 18.54$, $P \leq 0.01$) or fear–contempt ($F_{1,6} \geq 11.78$; $P < 0.05$).

In the course of these measurements we also discovered large individual differences in the category boundaries chosen during the pre-adaptation settings, and these appeared to be related to the categories to which the observers themselves belonged. This is

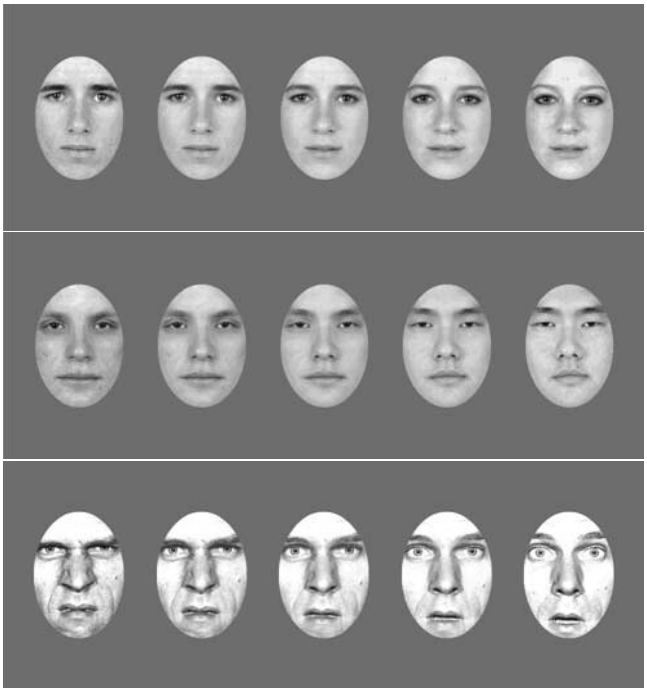

Figure 1 Examples of face pairs for the dimensions of gender (top row), ethnicity (middle row), or expression (bottom row). Morph arrays consisted of 100 images spanning the two original faces, which were assigned a value of 0 or 100. The morph level (for example, 25, 50, or 75) therefore corresponded to how far along the sequence the image fell between the two originals. Category boundaries corresponded to the image level chosen as the neutral point within the morph sequence.

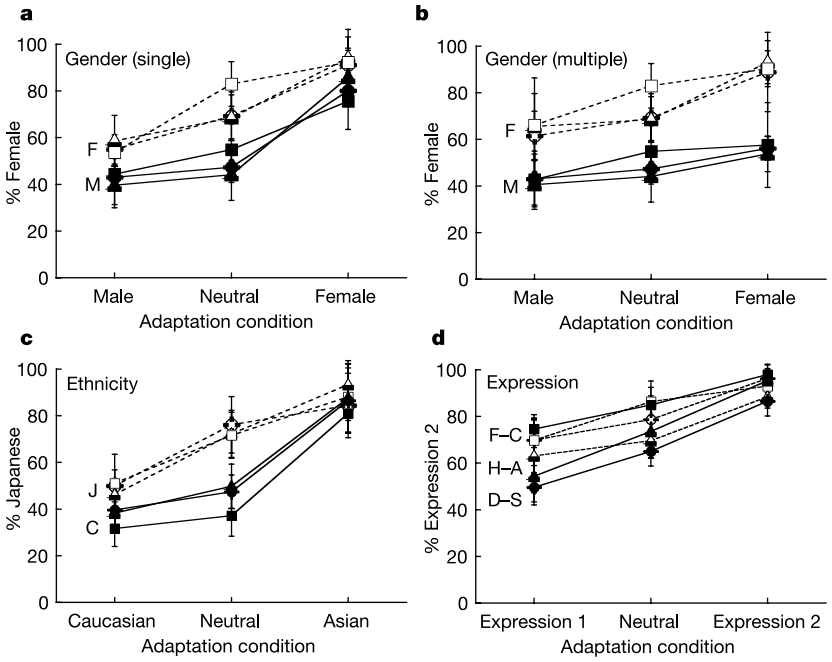

Figure 2 Category boundaries before or after adaptation. Each plot shows mean boundaries (±1 standard error) set by two observers for three face pairs, before or after viewing images from the two categories defining the morphs. **a**, Settings by a female (F) or male (M) for gender morphs. **b**, Settings by the same observers after adapting to a series of different male or female faces. **c**, Settings by a Japanese (J) or Caucasian (C) observer for ethnicity morphs. **d**, Boundaries selected by a Caucasian female (open symbols) and male (filled symbols) for morphs between happy–angry (H–A, triangles), disgust–surprise (D–S, circles) or fear–contempt (F–C, squares).

evident for the gender settings for the female and male subject in Fig. 2a. Females and males tended to choose gender boundaries in a male–female continuum that were shifted towards their own gender. We verified this for a set of 28 undergraduate students who set the gender boundaries under neutral adaptation. The average boundary for females (mean = 72, $n = 15$) and males (mean = 39, $n = 13$) (see Fig. 1 legend for an explanation of the mean value) differed by 33 steps in the image arrays, a difference that was again highly significant ($t = 14.08$, degrees of freedom (d.f.) = 26, $P < 0.001$) and perceptually obvious (Fig. 4a). To test whether this was due to a difference in decision strategies for the two genders (for example, females choosing the female side of a gender-neutral region and males choosing the male side of the same region) we repeated the measurements for a new group of ten female and nine male observers who were all instructed to respond to whether the face appeared 'female' or 'not female' (Fig. 4a). These settings did not differ from the previous group ($t = 0.81$, d.f. = 23, NS for females; $t = 0.81$, d.f. = 20, NS for males) while the differences between females and males within this second group were again large (mean = 68 versus 36; $t = 5.46$, d.f. = 17, $P < 0.001$). These differences suggest that observers may generally be more sensitive to how a face differs from their own category, although the extent to which this reflects differences in perception or criteria remains uncertain.

We next tested whether similar differences in category boundaries might occur for observers that differ in ethnicity. Boundary images for Japanese–Caucasian morphs were obtained for 38 Caucasian undergraduates in Reno, Nevada, and for 42 Japanese exchange students who had recently arrived for study in Reno. The latter group was tested within two weeks of their departure from Japan. The mean boundaries chosen were again very different for the two groups (67 versus 42; $t = 9.80$, d.f. = 78, $P < 0.001$) and were consistent with an increased sensitivity to how the faces differed from the observer's own ethnicity (Fig. 4b).

The differences between the Japanese and Caucasian students prompted us to test for signs of adaptive adjustments outside the

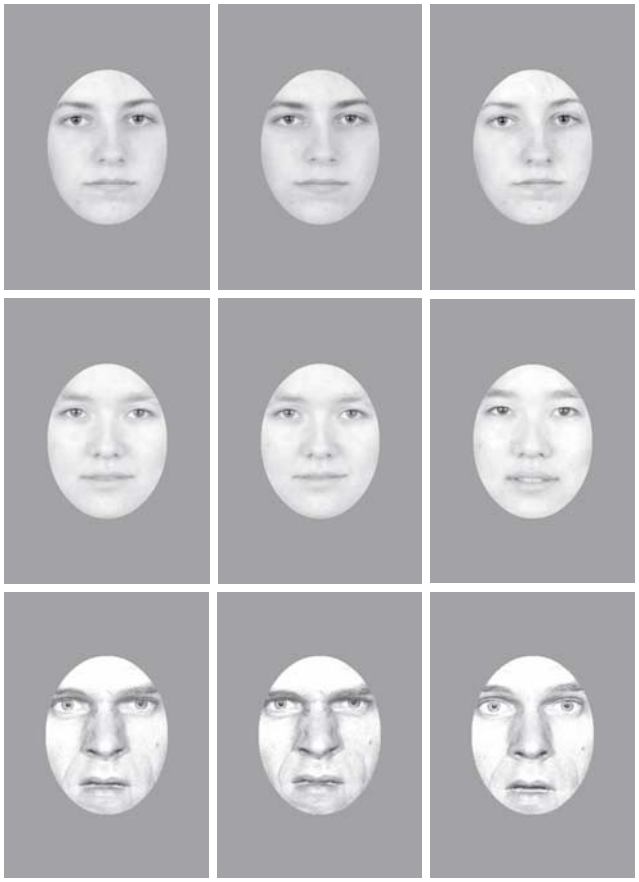

Figure 3 Examples of the face images chosen as category boundaries. Rows show boundary images before (left column) or after adaptation to gender (top row: male adapted, middle; female adapted, right), ethnicity (middle row: Caucasian adapted, middle; Japanese adapted, right), or expression (bottom row: disgust adapted, middle; surprise adapted, right).

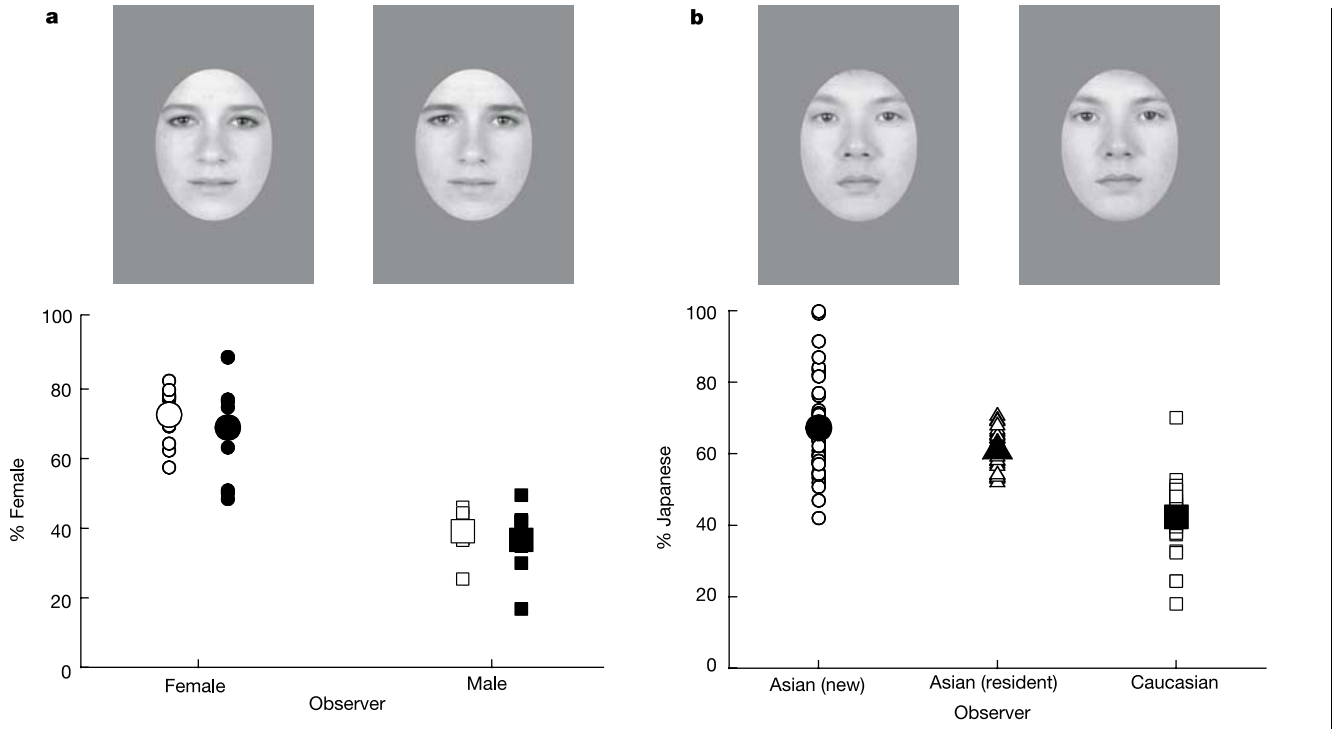

Figure 4 Category boundaries selected by different categories of observers. **a**, Gender boundaries. Open symbols show settings by females (circles) or males (squares) based on a male–female response criterion. Faces corresponding to the group means (enlarged symbols) are shown in the images above. Filled symbols show settings when observers set the gender boundary based on a female or not-female criterion. **b**, Ethnicity boundaries chosen by Asian students that had newly arrived in Reno, Nevada (circles) or were resident for at least one year (triangles), or for Caucasian students (squares). Faces show the mean images for the newly arrived Asian or for the Caucasian students.

controlled conditions of the laboratory, which could arise if observers are exposed to a change in the sample of faces encountered in their routine daily activities. To test this we measured ethnicity boundaries for a second group of 32 Asian and predominantly Japanese students who had been resident in the US for at least 1 yr. Their settings (mean = 61) were modestly but significantly shifted towards the neutral points for the Caucasian students (Fig. 4b), as confirmed by a *t*-test and (because the samples had very different variances) by a nonparametric Wilcoxon signed ranks test ($Z = -1.81$; $P < 0.05$ one-tailed). Questionnaires administered to a subset from this group revealed that their settings were also negatively correlated with the length of their stay in the United States ($r = -0.57$, $n = 20$, $P < 0.01$), while positively correlated with self-reports of the percentage of time that they spent with individuals of the same ethnicity ($r = 0.59$, $n = 20$, $P < 0.01$). That is, the perceptual boundaries tended to shift more the longer these students were in the United States and the more they interacted with Caucasian individuals. A complete shift may be unlikely, because the gender differences suggest that observers may remain more sensitive to how faces differ from their own facial categories. The role of contact in the 'other race effect' for face perception has been widely investigated but remains poorly understood[16,17]. Our short-term adaptation effects suggest that one component of long-term contact with a new population may include actual changes in the appearance of faces induced by adaptation.

Variability among faces is obviously a fundamentally important source of information about individual and group identities and the long-term (for example, age) and short-term (for example, emotional) states of an individual. Yet because this variation is not random or uniform we are all exposed to a different diet of faces. Our results suggest that these natural stimulus variations are potentially large enough to induce different states of adaptation in observers, states that may influence strongly how faces are perceived and interpreted. Adaptation is thought to facilitate efficient coding of low-level stimulus features by normalizing visual responses to the average stimulus levels in scenes, and aids perceptual constancy by discounting variations in both the environment and the observer. Adapting face perception to the average characteristics of the distribution of faces that an individual encounters may similarly be important for calibrating the visual processes encoding faces. □

Methods

Stimuli were frontal-view images of individual faces taken from the JACNeuF and JACFEE image set of ref. 18. The images were converted to greyscale and cropped by a uniform oval (420 by 630 pixels) that preserved the internal features of the face while removing differences in external features of the head, such as hair shape. Pairs of images were then morphed with the program Gryphon Morph, with the morphing sequence stored as 100 frames of a movie file. On each trial an individual frame from the continuum was shown for 500 ms on a computer screen. The face subtended roughly 10° vertical and was displayed on a uniform grey background. Observers used a button box to make a two-alternative forced-choice response to classify the image into one of two categories (corresponding to morphs between two genders, ethnicities, or expressions). Successive images were then varied in two randomly interleaved staircases (that is, with the morph level presented on each trial stepped up or down depending on the response for the preceding trial) of 12 reversals each to estimate the stimulus level for each category boundary. On adaptation trials, subjects first viewed either of the two original images for 180 s, and then for 5 s between each test presentation until the staircases completed. Test and adapting images were separated by 250-ms intervals during which the screen remained uniform grey. In pre-adaptation trials, the uniform background was also shown during the adaptation intervals. Observers were asked to attend to the images throughout but were not otherwise given specific fixation instructions. Four repeated settings were made for three different face pairs for each stimulus category. Five subjects were tested for each condition, and included two of the authors (D.K. and Y.M.) and three naive observers who were unaware of the specific aims of the experiment. Procedures were approved by the Institutional Review Board of the University of Nevada and informed consent was obtained for all subjects.

Received 11 November 2003; accepted 5 February 2004; doi:10.1038/nature02420.

1. Webster, M. A. & MacLin, O. H. Figural after-effects in the perception of faces. *Psychon. Bull. Rev.* **6,** 647–653 (1999).
2. Leopold, D. A., O'Toole, A. J., Vetter, T. & Blanz, V. Prototype-referenced shape encoding revealed by high-level aftereffects. *Nature Neurosci.* **4,** 89–94 (2001).

3. Zhao, L. & Chubb, C. F. The size-tuning of the face-distortion aftereffect. *Vision Res.* **41,** 2979–2994 (2001).
4. Rhodes, G., Jeffery, L., Watson, T. L., Clifford, C. W. G. & Nakayama, K. Fitting the mind to the world: Face adaptation and attractiveness aftereffects. *Psychol. Sci.* **14,** 558–566 (2003).
5. Watson, T. L. & Clifford, C. W. G. Pulling faces: An investigation of the face-distortion aftereffect. *Perception* **32,** 1109–1116 (2003).
6. Moscovitch, M., Winocur, G. & Behrmann, M. What is special about face recognition? Nineteen experiments on a person with visual object agnosia and dyslexia but normal face recognition. *J. Cogn. Neurosci.* **9,** 555–604 (1997).
7. Farah, M. J., Wilson, K. D., Drain, M. & Tanaka, J. N. What is "special" about face perception? *Psychol. Rev.* **105,** 482–498 (1998).
8. Kanwisher, N. Domain specificity in face perception. *Nature Neurosci.* **3,** 759–763 (2000).
9. Diamond, R. & Carey, S. Why faces are and are not special: An effect of expertise. *J. Exp. Psychol. Gen.* **115,** 107–117 (1986).
10. Gauthier, I. & Tarr, M. J. Becoming a "Greeble" expert: Exploring mechanisms for face recognition. *Vision Res.* **37,** 1673–1682 (1997).
11. Etcoff, N. L. & Magee, J. J. Categorical perception of facial expression. *Cognition* **44,** 227–240 (1992).
12. Beale, J. M. & Keil, F. C. Categorical effects in the perception of faces. *Cognition* **57,** 217–239 (1995).
13. McKone, E., Martini, P. & Nakayama, K. Category perception of face identity in noise isolates configural processing. *J. Exp. Psychol. Hum. Percept. Perform.* **27,** 573–599 (2001).
14. Ekman, P. Strong evidence for universals in facial expression: A reply to Russell's mistaken critique. *Psychol. Bull.* **115,** 268–287 (1994).
15. Young, A. *et al.* Facial expression megamix: tests of dimensional and category accounts of emotion recognition. *Cognition* **63,** 271–313 (1997).
16. Levin, D. T. Race as a visual feature: Using visual search and perceptual discrimination tasks to understand face categories and the cross-race recognition deficit. *J. Exp. Psychol. Gen.* **129,** 559–574 (2000).
17. Furl, N., Phillips, P. J. & O'Toole, A. J. Face recognition algorithms and the other-race effect: computational mechanisms for a developmental contact hypothesis. *Cogn. Sci.* **26,** 797–815 (2002).
18. Matsumoto, D. & Ekman, P. *Japanese and Caucasian Facial Expressions of Emotion (JACFEE) and Neutral Faces (JACNeuF)* (Department of Psychology, San Francisco State Univ., San Francisco, 1988).

Acknowledgements This work was supported by the National Eye Institute.

Competing interests statement The authors declare that they have no competing financial interests.

Correspondence and requests for materials should be addressed to M.A.W. (mwebster@unr.nevada.edu).

A DNA vaccine induces SARS coronavirus neutralization and protective immunity in mice

Zhi-yong Yang[1]*, Wing-pui Kong[1]*, Yue Huang[1], Anjeanette Roberts[2], Brian R. Murphy[2], Kanta Subbarao[2] & Gary J. Nabel[1]

[1]*Vaccine Research Center, NIAID, National Institutes of Health, Building 40, Room 4502, MSC-3005, 40 Convent Drive, Bethesda, Maryland 20892-3005, USA*
[2]*Laboratory of Infectious Diseases, NIAID, National Institutes of Health, MSC-8007, 50 South Drive, Bethesda, Maryland 20892-8007, USA*

* These authors contributed equally to this work

Public health measures have successfully identified and contained outbreaks of the severe acute respiratory syndrome (SARS) coronavirus (SARS-CoV)[1–5], but concerns remain over the possibility of future recurrences. Finding a vaccine for this virus therefore remains a high priority. Here, we show that a DNA vaccine encoding the spike (S) glycoprotein of the SARS-CoV induces T cell and neutralizing antibody responses, as well as protective immunity, in a mouse model. Alternative forms of S were analysed by DNA immunization. These expression vectors induced robust immune responses mediated by CD4 and CD8 cells, as well as significant antibody titres, measured by enzyme-linked immunosorbent assay. Moreover, antibody responses in mice vaccinated with an expression vector encoding a form of S that includes its transmembrane domain elicited neutralizing antibodies. Viral replication was reduced by more than six orders of magnitude in the lungs of mice vaccinated with these S plasmid DNA expression vectors, and protection was mediated by a humoral but not a T-cell-dependent immune mechanism. Gene-based vaccination for the SARS-CoV elicits effective immune responses that generate protective immunity in an animal model.

The SARS-CoV emerged in Asia as a highly aggressive pathogen that can be lethal in adults and the elderly[1–6]. Although its genetic organization is similar to other coronaviruses, recent phylogenetic studies suggest that it may be most closely related to type II coronaviruses[7–9]. Previously described coronaviruses have not usually induced lethal disease in humans, but their pathogenicity in domestic animal species has been well documented[10], and experimental vaccines developed for animals have provided insight into mechanisms of protective immunity[11,12]. Studies of the immune response to coronaviruses suggest that both cell-mediated and humoral immunity contribute to long-term protection[13,14].

To discover the gene products and mechanisms of protective immunity relevant to SARS-CoV, two sets of cDNAs encoding the SARS-CoV S glycoproteins were prepared using modified codons to optimize expression and to minimize recombination with endogenous coronaviruses. Because coronaviruses assemble in the compartment between the endoplasmic reticulum (ER) and Golgi apparatus[10], and the S leader may direct it to the ER, the native leader sequence was retained in one set of vectors (Fig. 1a) and replaced in another set with a leader sequence derived from the interleukin-2 gene. Expression was not significantly altered by this leader sequence substitution (data not shown), and it was not studied further. Two S carboxy-terminal mutants, one that truncated the cytoplasmic domain (SΔCD) and another that deleted the transmembrane and cytoplasmic regions (SΔTM), were prepared, and expression of these cDNAs by a mammalian expression vector suitable for human vaccination was confirmed (Fig. 1b).

The plasmids encoding these modified S glycoproteins were analysed for their ability to elicit antiviral immunity after intramuscular injection in BALB/c mice. Injection of S, SΔTM and SΔCD expression vectors induced a substantial immune response. A marked increase was observed in the number of SARS-CoV S-specific CD4 T-cell immune responses (Fig. 2a), as measured by intracellular cytokine staining for interferon-γ (IFN-γ) and tumour necrosis factor-α (TNF-α). In addition, substantial SARS-CoV S-specific CD8 cellular immunity was detected at levels at least sevenfold above the background response. Humoral immunity was initially

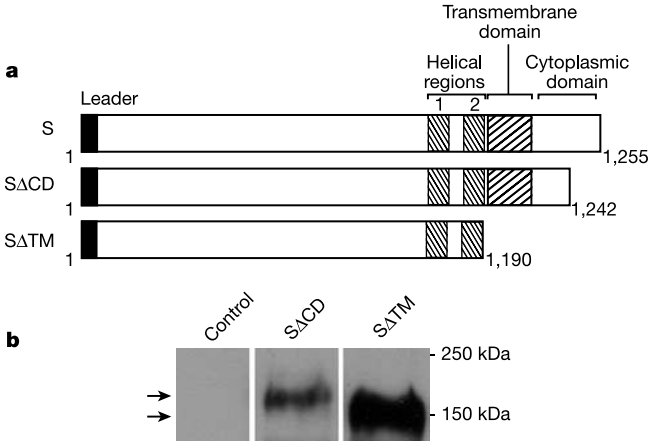

Figure 1 Schematic representation of SARS-CoV glycoprotein cDNAs and expression of recombinant proteins. **a**, The structure of the cDNAs used. **b**, Expression of these constructs, determined by western blot analysis with antisera reactive with SARS-CoV S, was evaluated after transfection of the indicated plasmid expression vectors in 293T cells. Arrows indicate specific SΔCD (upper) and SΔTM (lower) bands.